© 2014. Published by The Company of Biologists Ltd | Development (2014) 141, 3900-3909 doi:10.1242/dev.105718

RESEARCH ARTICLE

Lhx3 and Lhx4 suppress Kolmer–Agduhr interneuron characteristics within zebrafish axial motoneurons

Steve Seredick*,, Sarah A. Hutchinson‡,**, Liesl Van Ryswyk§, Jared C. Talbot¶ and Judith S. Eisen‡‡**

ABSTRACT

A central problem in development is how fates of closely related cells are segregated. Lineally related motoneurons (MNs) and interneurons (INs) express many genes in common yet acquire distinct fates. For example, in mouse and chick Lhx3 plays a pivotal role in the development of both cell classes. Here, we utilize the ability to recognize individual zebrafish neurons to examine the roles of Lhx3 and its paralog Lhx4 in the development of MNs and ventral INs. We show that Lhx3 and Lhx4 are expressed by post-mitotic axial MNs derived from the MN progenitor (pMN) domain, p2 domain progenitors and by several types of INs derived from pMN and p2 domains. In the absence of Lhx3 and Lhx4, early-developing primary MNs (PMNs) adopt a hybrid fate, with morphological and molecular features of both PMNs and pMN-derived Kolmer–Agduhr′ (KA′) INs. In addition, we show that Lhx3 and Lhx4 distinguish the fates of two pMN-derived INs. Finally, we demonstrate that Lhx3 and Lhx4 are necessary for the formation of late-developing V2a and V2b INs. In conjunction with our previous work, these data reveal that distinct transcription factor families are deployed in post-mitotic MNs to unequivocally assign MN fate and suppress the development of alternative pMN-derived IN fates.

KEY WORDS: Zebrafish, Motoneuron, Interneuron, Kolmer–Agduhr, V2a, V2b, Lhx3, Lhx4

INTRODUCTION

Progressive restriction of cell fate during development is a complex process that requires coordinated changes in gene expression. After terminal division of progenitors, unique combinations of transcription factors promote acquisition of post-mitotic characteristics that define individual cell types. However, cells closely related by lineage share a common regulatory history and express many of the same transcription factors. This is particularly true in the vertebrate ventral spinal cord, where different types of neurons derive from a single progenitor domain specified by a common set of transcription factors (Lewis, 2006).

To understand how the fates of closely related neurons are specified, we examined derivatives of the progenitor of motoneuron (pMN) domain in the zebrafish ventral spinal cord. The zebrafish pMN lineage is well-characterized and generates several alternative neuron classes (Park et al., 2004). Analysis of these neuron classes is simplified because each spinal hemisegment has only a few neuron types, the development of which can be followed in intact embryos (Fig. 1) (Lewis and Eisen, 2003; McLean and Fetcho, 2008). Between 9 and 15 h post fertilization (hpf), the pMN domain generates 3-4 early-born primary MNs (PMNs) (Myers et al., 1986), as well as two interneurons (INs), Kolmer–Agduhr′ (KA′) and ventral-longitudinally descending (VeLD) (Park et al., 2004), within each spinal hemisegment. Both PMNs and these two INs can be identified by soma position, axon morphology and gene expression (Bernhardt et al., 1990, 1992; Kuwada et al., 1990). After 15 hpf, the pMN domain generates additional cell types: smaller, more numerous secondary MNs (SMNs); oligodendrocyte precursors; and a third class of INs, circumferentially descending (CiD) (Park et al., 2004). CiDs are morphologically and molecularly similar to excitatory V2a INs that arise from the dorsally adjacent p2 progenitor domain later in development (Batista et al., 2008; Kimura et al., 2008). At early stages these cells can be distinguished because CiDs are *olig2*-positive, whereas V2a INs are *vsx1*-positive (Kimura et al., 2006; Park et al., 2004). As in amniote vertebrates, zebrafish p2 progenitors also generate inhibitory V2b INs (Batista et al., 2008; Kimura et al., 2008).

After their terminal divisions, pMN-derived neurons express unique combinations of transcription factors from three different families. PMNs and SMNs are Islet^{+} Mnx^{+} Lhx3^{+}; VeLDs are Islet^{-} Mnx^{+} Lhx3^{+}; CiDs are Islet^{-} Mnx^{-} Lhx3^{+}; KA′s are Islet^{-} Mnx^{-} Lhx3^{-} (Batista et al., 2008; Hutchinson and Eisen, 2006; Kimura et al., 2006; Seredick et al., 2012). Knockdown of either Islet or Mnx family members compromises aspects of MN identity, and PMNs acquire features of specific pMN-derived INs. For example, in the absence of Islet proteins, PMNs aberrantly express GABA and have ipsilaterally descending axons in the ventral longitudinal fasciculus, characteristic of VeLDs (Hutchinson and Eisen, 2006). By comparison, in the absence of Mnxs, one PMN subtype aberrantly expresses *vsx2* and *vglut* and often has ipsilaterally descending axons in the lateral neuropil, which are characteristics of CiDs (Seredick et al., 2012). These results suggest that different transcription factor families expressed in post-mitotic MNs are dedicated to suppressing specific alternative IN programs within MNs. This prompted us to test the hypothesis that in PMNs, Lhx family members suppress characteristics of the remaining pMN-derived IN, KA′.

Lhx3 is an LIM homeodomain transcription factor that plays pivotal roles in MN and IN fates during neural development in both vertebrates and invertebrates (Thaler et al., 2002; Thor et al., 1999). In vertebrates, genome duplication created an Lhx3 paralog, Lhx4, that can substitute for Lhx3 in formation of V2a- and MN-promoting complexes (Gadd et al., 2011). Although mouse knockouts of either *Lhx3* or *Lhx4* are perinatally lethal (Li et al., 1994; Sheng et al., 1996), MNs are generated normally (Sharma

Institute of Neuroscience, 1254 University of Oregon, Eugene, OR 97403, USA. *Present address: Zymeworks Inc., 540-1385 West 8th Avenue, Vancouver, British Columbia, Canada V6H 3V9. ‡Present address: Program in Developmental & Stem Cell Biology, PGCRL, 686 Bay Street #15.9.410, Toronto, Ontario, Canada M5G 0A4. §Present address: Department of Biology, Pacific University, 2043 College Way, Forest Grove, OR 97116, USA. ¶Present address: Department of Molecular Genetics, The Ohio State University, 125 Rightmire Hall, 1060 Carmack Road, Columbus, OH 43210, USA.
**These authors contributed equally to this work

‡‡Author for correspondence (eisen@uoneuro.uoregon.edu)

Received 5 November 2013; Accepted 12 August 2014

Development (2014) 141, 3900-3909 doi:10.1242/dev.105718

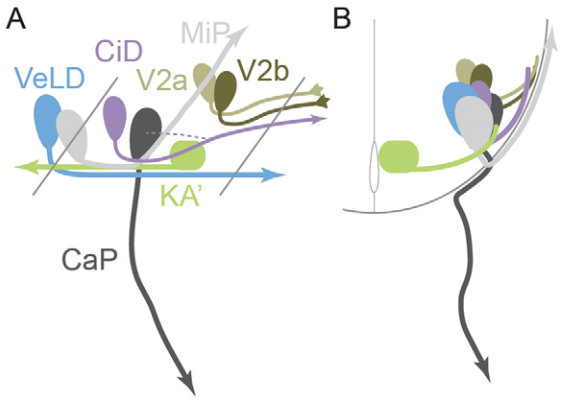

Fig. 1. Neuronal subtypes of zebrafish ventral spinal cord. Lateral (A) and cross-section (B) views of neurons in one spinal hemisegment. KA′s express Gad, have ascending axons and contact the ventricular lumen. Somata of all other neurons are laterally positioned. Two PMNs are shown: MiPs innervate dorsal myotome and CaPs innervate ventral myotome. VeLDs express Gad and have descending, ventromedial axons. CiDs, V2as and V2bs have descending, dorsolateral axons and can be distinguished from each other by marker expression and domain of origin (see main text). Later, some CiDs develop ascending collaterals, indicated by dashed line in A.

et al., 1998). However, at cervical levels, MN subtype identity is altered in the combined absence of Lhx3 and Lhx4. Cervical MNs, the axons of which normally exit ventrally, acquire features of spinal accessory column (SAC) MNs, and their axons exit dorsally (Sharma et al., 1998). Importantly, the fate of MNs at other axial levels remains unknown. Despite intensive investigation of Lhx3 involvement in regulatory networks that promote MN, V2a and V2b fates (Joshi et al., 2009; Lee et al., 2012, 2008, 2009; Lee and Pfaff, 2003; Thaler et al., 2002), it remains untested whether Lhx3 or Lhx4 is necessary for ventral spinal cord IN specification.

Here, we show that zebrafish Lhx4 is expressed, like Lhx3, in MNs and INs derived from both pMN and p2 domains. Morpholino oligonucleotide (MO) knockdown of Lhx3 and Lhx4 revealed that, at thoracic levels, many cells fated to become MNs aberrantly acquire characteristics of KA′ INs. In addition, overexpression of Lhx3 in pMN-derived neurons and progenitors causes an increase in CiDs at the expense of KA′s. Moreover, Lhx3 and Lhx4 are necessary for specification of many late-developing V2a and V2b INs. These findings provide new evidence of roles for Lhx3 and Lhx4 in the fates of specific ventral spinal cord INs and demonstrate that these Lhx proteins suppress a competing KA′ IN program within both trunk level axial MNs and pMN-derived CiD INs.

RESULTS

Lhx3 and Lhx4 are expressed in MNs, ventral INs and p2 progenitors

Zebrafish *lhx3* is expressed in pMN-derived PMNs, SMNs, VeLDs and CiDs (Appel et al., 1995; Batista et al., 2008), whereas KA′s are not reported to express *lhx3*. Lhx3 and Lhx4 cooperate to promote MN identity in mouse (Sharma et al., 1998); however, Lhx4 was uncharacterized in zebrafish. Thus, we determined the *lhx4* expression pattern on embryos of various stages and compared it with *lhx3*. *lhx4* expression begins at 11 hpf, the same time as *lhx3* (Fig. 2A,B). Like *lhx3*, *lhx4* is expressed in two medial cell stripes in the region that will form the ventral spinal cord. At 24 hpf, *lhx4* is expressed in fewer cells than *lhx3* (Fig. 2C,D). To understand the relationship between *lhx3* and *lhx4* expression, we assayed them simultaneously in *Tg(nrp1a:GFP)* embryos that label MNs (Sato-Maeda et al., 2008). At 16 hpf, all *lhx4*-expressing spinal cord cells co-express *lhx3*, whereas some *lhx3*-expressing cells do not express *lhx4* (Fig. 2E, arrowheads). The position of these cells relative to the *nrp1a:GFP* transgene suggests that they are primarily pMN-derived MNs and INs that also express *lhx3* (Appel et al., 1995). At 20 hpf, *lhx3* and *lhx4* are co-expressed in more dorsal cells. The relative locations of these more dorsally located co-expressing cells suggest they are p2-derived INs that express *lhx3* (Batista et al., 2008; Kimura et al., 2008). At 24 and 28 hpf, *lhx3* and *lhx4* appear to be almost entirely co-expressed (Fig. 2G,H). Thus, at these stages, *lhx4*, like *lhx3*, is expressed in MNs as well as in pMN- and p2-derived INs. In addition, *lhx4* is expressed in the pituitary and in a set of dorsal INs between the eyes (supplementary material Fig. S1). *lhx4* expression in the pituitary is similar to that of *lhx3*; however, the dorsal IN population that expresses *lhx4* does not express *lhx3*.

To examine expression of Lhx3 and Lhx4 proteins, we generated polyclonal antibodies (see Materials and Methods; supplementary material Fig. S2). To confirm that Lhx4 is expressed in MNs, we compared expression patterns of embryos double-labeled with anti-Lhx4 and anti-Islet (Korzh et al., 1993). At 18 hpf, anti-Lhx4 antibody labeled exclusively Islet^{+} cells, suggesting that initially only PMNs express Lhx4 (Fig. 2J). By contrast, at 18 hpf many cells are Lhx3^{+}Islet^{-}, consistent with Lhx3 expression in VeLDs, CiDs and V2as (Fig. 2I, arrowhead) (Appel et al., 1995; Batista et al., 2008). By 24 hpf, Lhx3 and Lhx4 continued to be expressed in all Islet^{+} cells, indicating expression in all PMNs and at least some SMNs (Fig. 2K,L). At this time, anti-Lhx4 antibody labeled many Islet^{-} cells in the ventral spinal cord, consistent with Lhx4 expression expanding into VeLDs, CiDs and V2as. These data indicate that Lhx4, like Lhx3, is expressed in PMNs, SMNs, VeLDs, CiDs and V2as but is excluded from medially located KA′s (Fig. 2Q).

To examine whether Lhx3 and Lhx4 are expressed in spinal cord progenitors similar to mouse and chick (Sharma et al., 1998; Tsuchida et al., 1994), we co-labeled transgenic embryos expressing GFP in pMN or p2 progenitors with anti-Lhx3/4 antibodies and a mitotic marker, anti-phospho Histone H3 (P-H3). We identified pMN progenitors using *Tg(olig2:GFP)* embryos that express GFP in pMN progenitors and their post-mitotic derivatives (Shin et al., 2003). We found that GFP^{+} Lhx3/4^{+} cells in 12, 16 and 20 hpf *Tg(olig2:GFP)* embryos never co-expressed P-H3 (Fig. 2M and data not shown). We confirmed that Lhx3 and Lhx4 are excluded from pMN progenitors by labeling proliferating cells with 5-ethynyl-2′-deoxyuridine (EdU) at 11 hpf, the time of peak PMN generation (Myers et al., 1986). When processed at 12 hpf, no Lhx3/4^{+} cells had incorporated EdU (Fig. 2N,P). We identified p2 progenitors, using *Tg(vsx1:GFP)* embryos that express GFP in progenitors just prior to their final division as well as in V2 INs (Kimura et al., 2008). By contrast to pMN progenitors, at 20 hpf some p2 progenitors were Lhx3/4^{+} and P-H3^{+} (Fig. 2O,P). These data show that Lhx3 and Lhx4 are expressed by p2 progenitors but are absent from pMN progenitors, including KA′ progenitors.

Lhx3 and Lhx4 promote normal MN axon morphology

The altered axon projection patterns of cervical MNs in mouse embryos lacking Lhx3 and Lhx4 (Sharma et al., 1998) prompted us to examine zebrafish trunk MNs in the absence of these proteins. We labeled MO-injected embryos with zn1 and anti-Syt2b antibodies that reveal axons of two PMN subtypes, ventrally projecting caudal primary (CaP) and dorsally projecting middle primary (MiP) (Melancon et al., 1997; Myers et al., 1986;

Development (2014) 141, 3900-3909 doi:10.1242/dev.105718

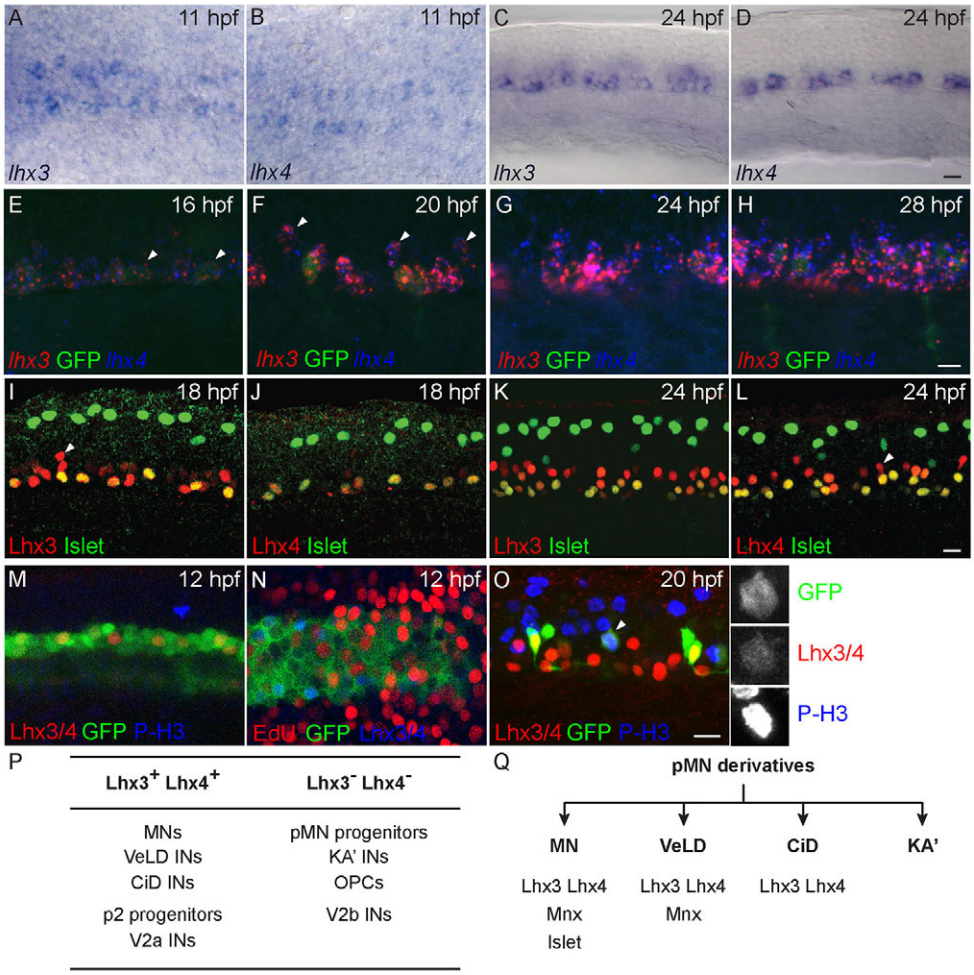

Fig. 2. *lhx4* and *lhx3* are expressed in many cells in the ventral neural tube. All images oriented with anterior to the left. (A,B) Dorsal view of 11 hpf embryos. Both *lhx3* (A) and *lhx4* (B) are expressed beginning at 11 hpf in two medial cell stripes. (C,D) Lateral view of spinal cord adjacent to somites 8-12 of 24 hpf embryo. Both *lhx3* (C) and *lhx4* (D) are expressed in the pMN domain; however, *lhx4* is expressed in fewer cells than *lhx3*. (E-H) *lhx3* and *lhx4* expression in ventral neural tube of *Tg(nrp1a:GFP)* embryos. (E) At 16 hpf, *lhx3* and *lhx4* are expressed at the dorsoventral level of GFP^+ MNs, whereas some GFP^+ cells express only *lhx3* (arrowheads). (F) At 20 hpf, *lhx3* and *lhx4* expression has expanded to include more dorsal GFP^- cells (arrowheads). (G,H) At 24 hpf and 28 hpf, *lhx3* and *lhx4* are broadly co-expressed in GFP^+ and GFP^- cells throughout the lateral half of ventral spinal cord. (I-L) Lateral views of spinal cord hemisegments adjacent to somites 8-12 co-labeled for Islet and either Lhx3 or Lhx4. Dorsal $Islet^+$ cells are Rohon–Beard sensory neurons. Anti-Islet labels PMNs at 18 hpf, and PMNs plus a few SMNs at 24 hpf. (I) At 18 hpf, anti-Lhx3 labels all $Islet^+$ PMNs as well as slightly more dorsal cells (arrowhead) in ventral neural tube. (J) At 18 hpf, anti-Lhx4 labels almost exclusively $Islet^+$ PMNs. (K) By 24 hpf, anti-Lhx3 labels all $Islet^+$ PMNs and SMNs and an increased number of cells in ventral neural tube. (L) Anti-Lhx4 also labels all $Islet^+$ PMNs and SMNs in addition to other more dorsal cells (arrowhead) in ventral neural tube at 24 hpf. (M) Lateral view of 12 hpf *Tg(olig2:GFP)* embryo co-labeled with anti-Lhx3/4 and anti-phospho-Histone H3 (P-H3). (N) Dorsal view of 12 hpf *Tg(olig2:GFP)* embryo incubated with EdU from 11 hpf and labeled with EdU and anti-Lhx3/4. (O) Lateral view of 20 hpf *Tg(vsx1:GFP)* embryo co-labeled with anti-Lhx3/4 and anti-P-H3. Enlarged, single channel images of indicated cell (arrowhead) demonstrate co-expression. (P) Summary of Lhx3- and Lhx4-expressing cells in the ventral spinal cord. (Q) Combinatorial expression of three transcription factors that uniquely label all four neuronal derivatives of the zebrafish pMN domain. Scale bars: 20 µm.

Trevarrow et al., 1990). Injection of either *lhx3* or *lhx4* MO alone had modest to no effect on PMN axon formation (Fig. 3A-C,E). However, co-injection of *lhx3* and *lhx4* MOs severely reduced PMN axon numbers (Fig. 3D,E). Reduction was sporadic along the length of the trunk and in many cases differentially affected CaPs and MiPs within a single trunk segment. SMN development was also compromised. *lhx3* and *lhx4* MO-injected embryos lacked Alcama (Fashena and Westerfield, 1999) expression on SMN somata and fasciculated axons (Fig. 3F,G). Live imaging of *s1020t; Tg(UAS-E1b:Kaede)* embryos revealed that SMN axons projecting to dorsal and ventral axial muscles adjacent to trunk somites 5-15 were variably present at 48 hpf. Motor nerves that were present were much thinner, suggesting fewer SMN axons per nerve (Fig. 3H,I). By contrast to Lhx3- and Lhx4-deficient mouse cervical MNs (Sharma et al., 1998), axons of Lhx3- and Lhx4-deficient zebrafish trunk MNs that left the spinal cord invariably exited at the ventral root.

The loss of trunk MN axons following Lhx3 and Lhx4 knockdown prompted us to test whether these MNs ever formed. Lhx3 and Lhx4 knockdown resulted in normal numbers of $Islet^+$ trunk cells at 28 and 48 hpf, suggesting that both PMNs and SMNs are generated (Fig. 4A,C,G-J). This is similar to Lhx3 and Lhx4 mouse embryos in which cervical MNs are present, but have altered identities (Sharma et al., 1998). By contrast, Islet1 is required for Lhx3 and Lhx4 expression in mouse (Pfaff et al., 1996), whereas zebrafish Lhx3 and Lhx4 expression is unaffected by Islet1 knockdown (Fig. 4D,E). Together, these observations show that equivalent numbers of MNs are generated in the presence and absence of Lhx3

Development (2014) 141, 3900-3909 doi:10.1242/dev.105718

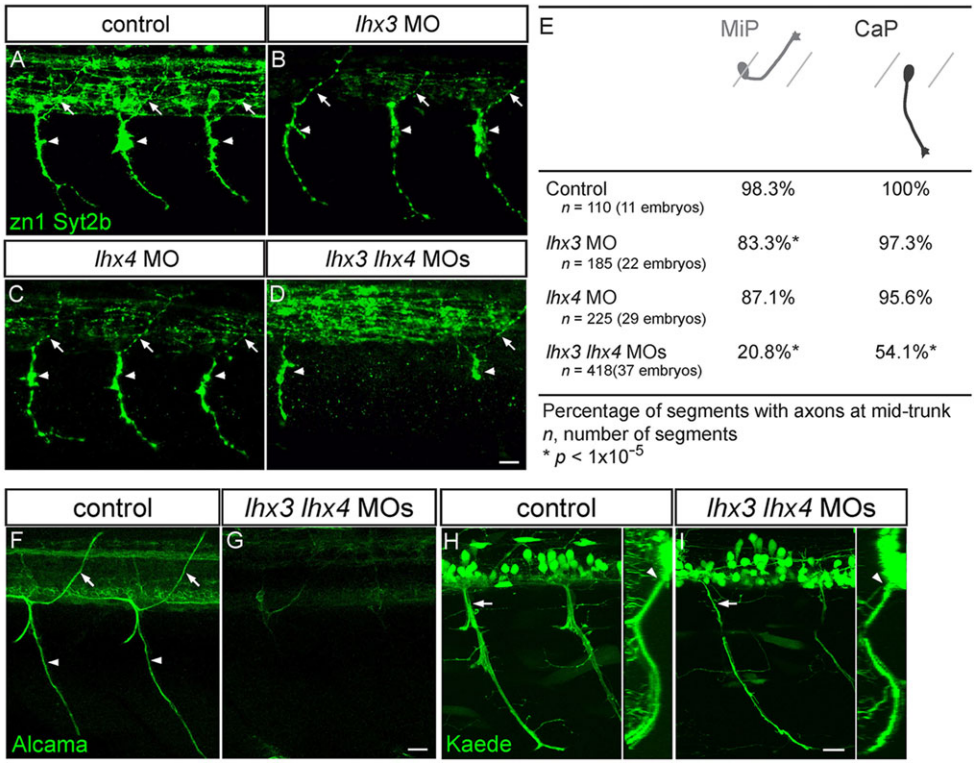

Fig. 3. Lhx3 and Lhx4 are required for normal PMN axon morphology. (A-D) Lateral views of 28 hpf embryos co-labeled with zn1 and anti-Syt2b. Control (A), *lhx3* MO-injected (B) and *lhx4* MO-injected (C) embryos have normal dorsal MiP axons (arrows) and ventral CaP axons (arrowheads). MiP, CaP, or MiP and CaP axons are often absent from *lhx3+lhx4* MO-injected embryos (D). Apparent variation in intraspinal labeling in B and C was a consequence of embryo orientation and does not reflect differences in IN axon labeling. (E) Quantification of MiP and CaP phenotypes in control and MO-injected embryos. (F,G) Lateral views of somites 8-12 of 72 hpf embryos labeled with anti-Alcama. Alcama labeling of SMN axons and somata was almost completely missing from embryos injected with *lhx3+lhx4* MOs. (H,I) Lateral views of 48 hpf *s1020t;Tg(UAS-E1b:Kaede)* embryos. Ventral nerves in *lhx3+lhx4* MO-injected embryos were thinner (arrows), yet exited through the ventral root (arrowhead); inset shows an optical cross-section. Scale bars: 20 µm.

and Lhx4 and suggest that, in zebrafish, Islet1 expression in trunk MNs is regulated independently of Lhx3 and Lhx4. These data are consistent with our previous results showing that, in the absence of Islet1, prospective zebrafish trunk MNs retain Lhx3 expression but differentiate as INs (Hutchinson and Eisen, 2006).

To confirm the specificity of our MO phenotype, we performed a mosaic rescue experiment by injecting *UAS:EGFP-P2A-lhx3* plasmid into the *s1020t* enhancer trap line in which GAL4VP16 is expressed under *olig2* control (Wyart et al., 2009). This allowed us to label cells overexpressing Lhx3 and to evaluate the proportion of labeled MNs. In control embryos, MNs comprised 55% of labeled neurons (Table 1), whereas in embryos injected with *lhx3* and *lhx4* MOs MNs comprised only 31% of labeled neurons. Co-expression of Lhx3 with EGFP restored the percentage of labeled MNs to 55%.

Lhx3 and Lhx4 prevent PMN acquisition of KA′ IN characteristics

The reduction of trunk motor projections in *lhx3+lhx4* MO-injected embryos led us to examine the phenotype of cells otherwise fated to become MNs. As the loss of Islet or Mnx results in hybrid PMNs with VeLD or CiD characteristics, respectively (Hutchinson and Eisen, 2006; Seredick et al., 2012), we hypothesized that PMNs in embryos lacking Lhx3 and Lhx4 would have characteristics of KA′s, the other pMN-derived IN. To test this, we co-labeled embryos with antibodies against Islet and Gad and found that, in the absence of Lhx3 and Lhx4, many Islet^{+} ventral spinal cord cells co-expressed Gad (Fig. 5A,B) and GABA (data not shown). These cells also expressed *chat* (*chata*, choline O-acetyltransferase a – Zebrafish Model Organism Database), which encodes the synthetic enzyme for acetylcholine, their normal transmitter (Fig. 5C,D). These results provide evidence that, in the absence of Lhx3 and Lhx4, PMNs develop a hybrid identity in which they express both MN and IN characteristics.

To resolve the identity of MN-IN hybrids, we labeled pMN-derived cells by injecting *UAS:EGFPCAAX* plasmid into *s1020t* embryos. This allowed us to visualize morphologies and proportions of MNs, VeLDs and KA′s. In addition to labeled MiPs, CaPs, VeLDs and KA′s seen in control embryos (Fig. 5E,F), in the absence of Lhx3 and Lhx4 we observed classes of aberrant axon projections. Notably, all aberrantly projecting neuron classes acquired ipsilaterally ascending axons, a hallmark of pMN-derived KA′s. There were two types of INs with axons that ascended through lateral spinal cord (ascending interneurons, aINs): most of these INs had a proximal axon that descended through the medial spinal cord before turning laterally and ascending through the lateral neuropil (Fig. 5G), although some aINs had axons that ascended through the spinal cord without a proximal descending segment (Fig. 5H). The laterally positioned somata of these neurons distinguished them from medially positioned KA′ somata. A second class of aberrant neurons had bifurcating spinal axons, one ascending and the other one descending (bifurcating interneurons, bINs; Fig. 5I). A third class had MN-IN hybrid morphologies (MN-aIN; Fig. 5J). These cells had motor projections into the ventral myotome as well as ascending IN axons. The aberrant neurons with ascending axons were probably transformed MNs, as there were fewer MNs without a significant increase in either KA′s or VeLDs (Fig. 5K).

Despite ectopic expression of Gad and GABA in MNs in the absence of Lhx3 and Lhx4 (Fig. 5 and data not shown), the total number of GABAergic cells in the ventral spinal cord was unchanged (control=10.0±2.0 GABA^{+} cells/hemisegment; *lhx3 lhx4* MOs=8.8±2.0 GABA^{+} cells/hemisegment). This observation raised the possibility that one or more types of pMN-derived IN failed to differentiate its normal transmitter phenotype in the absence of Lhx3 and Lhx4. VeLDs and KA′s are both GABAergic (Park et al., 2004). In *lhx3+lhx4* MO-injected embryos, VeLDs expressed GABAergic properties normally

Development (2014) 141, 3900-3909 doi:10.1242/dev.105718

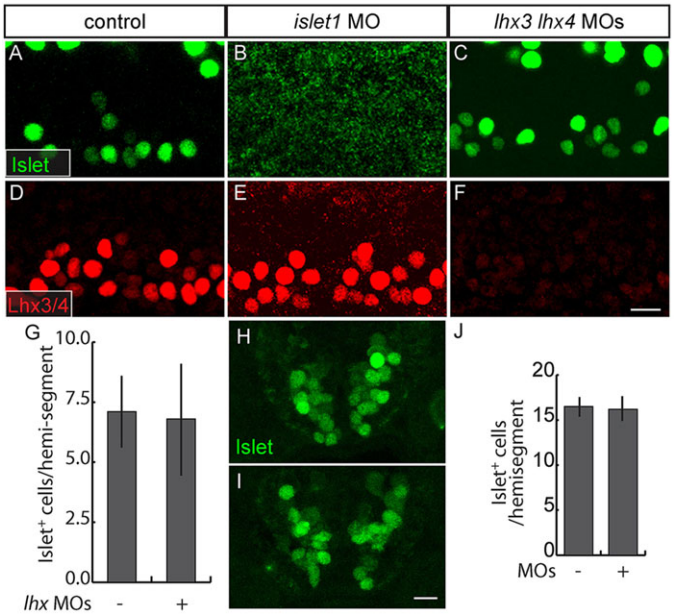

Fig. 4. Islet and Lhx3/4 proteins are independently regulated in ventral spinal cord. (A-F) Lateral views of 28 hpf embryos. MN Islet expression is absent from *islet1* MO-injected embryos (A,B), but persists in *lhx3+lhx4* MO-injected embryos (C). Lhx3/4 expression persists in *islet1* MO-injected embryos (D,E) and is absent from *lhx3+lhx4* MO-injected embryos (F). (G) Quantification of Islet$^+$ PMNs and early-born SMNs in presence or absence of Lhx3 and Lhx4 (P=0.18; control, n=56 spinal hemisegments in seven embryos; MOs, n=80 spinal hemisegments in ten embryos). (H,I) Sections of ventral spinal cord of 48 hpf embryos labeled with anti-Islet. Islet expression persists in embryos injected with *lhx3+lhx4* MOs. (J) Quantification of Islet$^+$ MNs in the presence or absence of Lhx3 and Lhx4 (P=0.44; n=10 alternating sections from ten embryos for both conditions). Scale bars: 20 µm.

(supplementary material Fig. S3), but far fewer KA′s expressed GABAergic properties (supplementary material Fig. S4). Because KA′s do not express *lhx3* or *lhx4*, we hypothesized that these genes might affect KA′ differentiation cell non-autonomously. Previous studies showed that Notch promotes KA′ identity (Shin et al., 2007) and that PMNs express Notch ligands (Appel and Eisen, 1998; Haddon et al., 1998); thus, Lhx3 and Lhx4 might regulate expression or presentation of Notch ligands in PMNs to promote Gad expression in KA′s. We tested this idea by overexpressing the Notch intracellular domain (NICD) and by blocking Notch activity with DAPT. Notch overexpression resulted in supernumerary GABAergic KA′s, and DAPT treatment diminished the number of GABAergic KA′s (supplementary material Fig. S4), as observed in previous studies. Consistent with our hypothesis, overexpressing NICD in *lhx3+lhx4* MO-injected embryos restored GABAergic KA′ numbers to wild-type levels. However, blocking Notch activity in *lhx3+lhx4* MO-injected embryos enhanced reduction of GABAergic KA′s (supplementary material Fig. S4). Together, these results suggest that, although both Notch and Lhx3 and Lhx4 affect KA′ differentiation, they do so through parallel pathways.

Lhx3 promotes CiD specification at the expense of KA′s

Our data suggest that Lhx3 and Lhx4 inhibit KA′ characteristics in PMNs; thus, we predicted that misexpression of *lhx3* would inhibit KA′ formation. To test this hypothesis, we injected *UAS:EGFP-P2A-lhx3* plasmid into *s1020t* embryos to drive Lhx3 expression in *olig2*-expressing cells (Wyart et al., 2009). In addition to the typical MNs, VeLDs and KA′s labeled in control embryos, we observed two classes of INs with aberrant morphologies. One class had an ipsilateral, descending axon that emerged from a ventromedial soma, a position characteristic of KA′s (dKA′s; Fig. 6A). The other class had an axon that emerged from a ventromedial soma and grew circumferentially before descending through the lateral neuropil. This class also had an ascending collateral that arose from the proximal portion of the main axon (CiD-KA′; Fig. 6B). This characteristic CiD axon morphology was not observed in control embryos, presumably because CiDs typically arise later than the time at which we assayed (Park et al., 2004). The aberrant INs with descending axons were probably transformed KA′s, as fewer KA′s formed without significant increases in the proportions of either MNs or VeLDs (Fig. 6C). These results demonstrate that Lhx3 is sufficient to inhibit KA′ fate and support the idea that Lhx3 specifies CiDs.

Lhx3 and Lhx4 promote formation of late-born V2 INs

Vertebrate p2 progenitors express Lhx3 and produce immature V2 INs that differentiate into two distinct types: V2as maintain Lhx3 expression, express Delta and differentiate as Vsx2$^+$ excitatory INs; V2bs extinguish Lhx3 expression and require Notch activity to differentiate as Tal1$^+$ Gata3$^+$ inhibitory INs (Batista et al., 2008; Del Barrio et al., 2007; Kimura et al., 2008; Lundfald et al., 2007; Peng et al., 2007). Lhx3 overexpression is sufficient to induce ectopic V2a formation in chick (Tanabe et al., 1998; Thaler et al., 2002), but whether Lhx3 and Lhx4 are necessary to promote V2 development remains untested.

To address this question, we knocked down Lhx3 and Lhx4 in *Tg(vsx1:GFP)* embryos and scored *vsx2* and *tal1* expression in GFP$^+$ neurons. At 24 hpf, we observed no difference in the number of V2a and V2b INs (Fig. 7A-D,K). However, in slightly older embryos we noticed a reduced number of *vsx2*$^+$ cells in the absence of Lhx3 and Lhx4 (data not shown). Thus, we examined the number of V2as and V2bs at 48 hpf, when many more are present, using a *Tg(vsx2:GFP)* line (Kimura et al., 2006) to score V2as, or labeling *Tg(vsx1:GFP)* embryos with *gata3* to identify V2bs. Whereas the number of immature *Tg(vsx1:GFP)* V2 neurons at 48 hpf was unchanged (Fig. 7I,J,M), the number of neurons expressing differentiated V2a and V2b markers was significantly reduced (Fig. 7E-H,L) by the absence of Lhx3 and Lhx4. These results suggest that Lhx3 and Lhx4 are dispensable for the earliest-born V2 INs, but are required for differentiation of later-born V2a and V2b INs.

DISCUSSION

Here, we have made three principal findings: first, Lhx3 and Lhx4 cooperate to inhibit a competing KA′ IN program within PMNs

Table 1. Lhx3 rescues the *lhx3 lhx4* MO-induced motor axon phenotype

	UAS-E1b:EGFP	*lhx3 lhx4* MOs *UAS-E1b:EGFP*	*lhx3 lhx4* MOs *UAS-E1b:EGFP-P2A-lhx3*
Percentage of EGFP$^+$ neurons with motor projections	54.6% (53/97 MNs, 15 embryos)	30.8% (25/81 MNs, 15 embryos)	55.3% (47/85 MNs, 17 embryos)

Development (2014) 141, 3900-3909 doi:10.1242/dev.105718

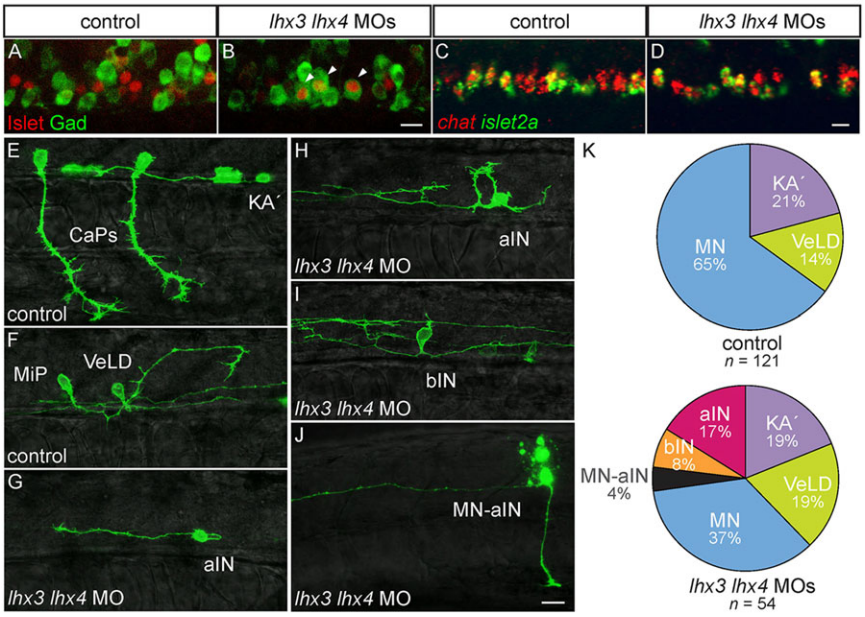

Fig. 5. Lhx3 and Lhx4 prevent PMNs from acquiring KA′ IN characteristics. (A-D) Lateral views of 24 hpf embryos. (A,B) Islet and Gad are co-expressed in *lhx3+lhx4* MO-injected embryos (arrowheads). (C,D) MNs continue to express *chat* in *lhx3+lhx4* MO-injected embryos. (E-I) Mosaically labeled pMN derivatives in 28-32 hpf *s1020t* embryos. (E,F) Injection of *UAS:EGFPCAAX* DNA labels PMNs, including both CaP (E) and MiP (F), as well as KA′ (E) and VeLD (F) in control embryos. (G-I) Mosaically labeled pMN derivatives in 28-32 hpf *s1020t* embryos injected with *lhx3* and *lhx4* MOs. (G) Aberrant neuron with an axon that initially projects caudally before turning laterally and ascending the spinal cord (aIN; *n*=9). (H) Aberrant neuron with axon that ascends without a proximal descending segment. (I) Aberrant neuron with bifurcating axons, one ascending and one descending (bIN; *n*=4). (J) Dye-labeled MN-IN hybrid neuron with both ascending IN and peripheral MN axons in embryo injected with *lhx3+lhx4* MOs (*n*=2); dye dorsal to the labeled neuron is from an adjacent cell killed during labeling. (K) Relative proportions of labeled pMN-derived neurons. Three new neuron classes appear in *lhx3+lhx4* MO-injected embryos; only MNs are under-represented relative to control embryos (P=2.2×10^{-5}). The percentage of labeled cells is listed for each condition. Scale bars: 20 µm.

(Fig. 8). Second, Lhx3 segregates alternative fates of two pMN domain-derived INs. Third, Lhx3 and Lhx4 are necessary for formation of late-developing V2 INs. We discuss each of these findings in turn.

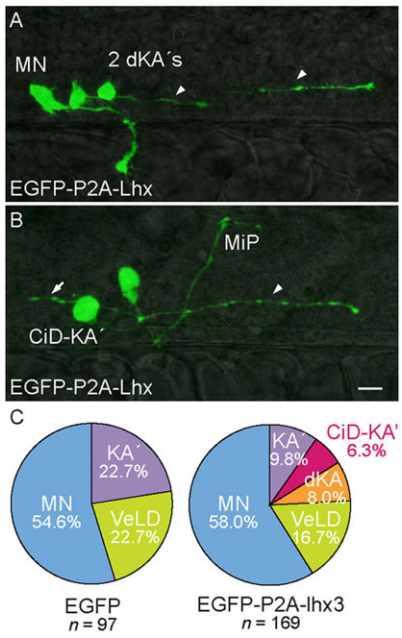

Fig. 6. Forced expression of Lhx3 in KA′s promotes descending and CiD axon trajectories. (A,B) Lateral views of 28 hpf *s1020t* embryos. Labeled pMN derivatives express EGFP-P2A-Lhx3. (A) Pair of aberrant ventromedially located KA′ neurons with descending axons (dKA′, arrowheads). A rostral primary (RoP) MN projecting to lateral muscle is also labeled. (B) Aberrant ventromedially located KA′ neuron with an axon that initially extends laterally before turning caudally and descending within the spinal cord (CiD-KA′, arrowhead). An ascending axon collateral (arrow) sprouts immediately adjacent to the intraspinal portion of a labeled MiP MN. (C) Relative proportions of labeled pMN-derived neurons. Two new IN classes appear in *UAS:EGFP-P2A-lhx3*-injected embryos; KA′s are under-represented relative to control embryos (P=1.6×10^{-5}). The percentage of labeled cells is listed for each condition. Scale bar: 20 µm.

Distinct transcription factor families suppress specific IN fates during PMN development

Lineage analysis revealed that PMNs and KA′s both derive from the pMN domain and can be siblings (Park et al., 2004). We determined that Lhx3 and Lhx4 act together to prevent PMNs from acquiring KA′ features, including transmitter expression and axonal projection.

Zebrafish MNs have an inherent propensity to acquire characteristics of pMN-derived INs. Knockdown of Islet1 results in excess VeLDs and eliminates motor projections (Hutchinson and Eisen, 2006), and knockdown of Mnxs causes MiP PMNs to acquire CiD features (Seredick et al., 2012). These results reveal the regulatory logic by which MN and pMN-derived IN fates are segregated (Fig. 8B): one family of transcription factors blocks each of the alternative pMN-derived IN programs in post-mitotic MNs. This mechanism efficiently resolves identities of distinct neurons, the fates of which diverge only after the final progenitor division.

Notably, knockdown of Lhx3 and Lhx4 does not result in a complete PMN-to-KA′ fate conversion. Resulting cells adopt a hybrid phenotype, expressing PMN markers while also acquiring KA′ characteristics, and in some cases even adopting a hybrid morphology. Formation of MN-IN hybrids is a consistent phenotype following knockdown of many zebrafish transcription factors, including those described above, as well as Nkx6.1 and Nkx6.2 (Hutchinson et al., 2007) and the Met receptor (Tallafuss and Eisen, 2008). These results suggest that none of these genes, with the possible exception of Islet, act as true master regulators of MN fate. Rather, each gene or gene family refines identity by suppressing the inherent potential of MNs to initiate genetic programs normally restricted to INs. Similar observations have been made in mouse. In *Runx1* mutant mice, a subset of brachial level MNs co-express Islet1 and the IN marker Pax2 (Stifani et al., 2008). In *Nkx6.1 Nkx6.2* double mutants, Islet1 and the IN marker Evx1 are transiently co-expressed (Vallstedt et al., 2001). In *Mnx1* knockout mice, MNs transiently co-express the V2a marker, Vsx2 (aka Chx10) (Arber et al., 1999; Thaler et al., 1999). Interestingly, Vsx2 binds to an *Mnx1* enhancer *in vivo* and blocks expression of an MN reporter *in vitro* (Lee et al., 2008), suggesting that a reciprocal strategy of

Development (2014) 141, 3900-3909 doi:10.1242/dev.105718

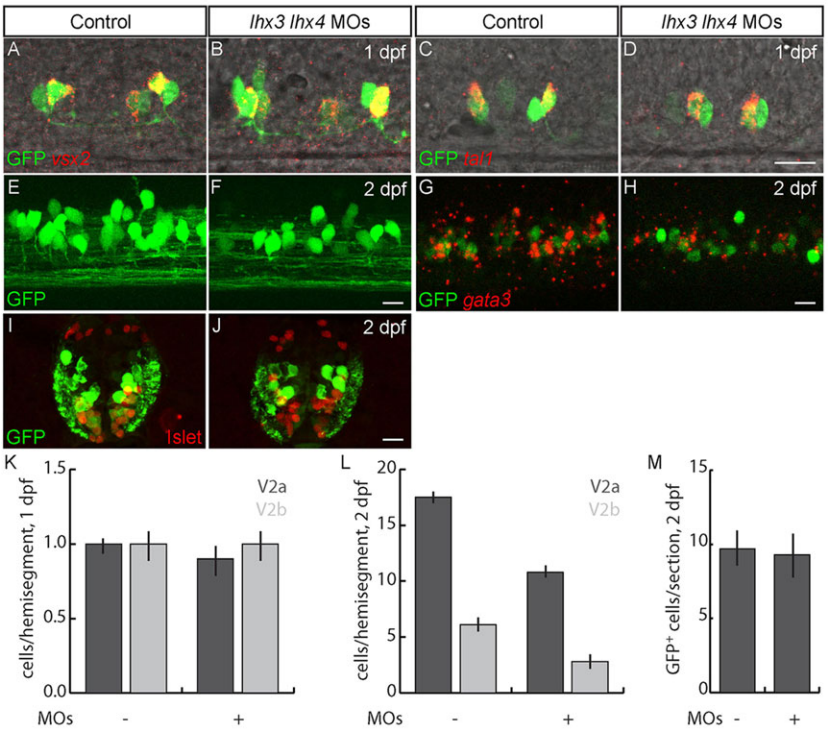

Fig. 7. Lhx3 and Lhx4 promote differentiation of late-born V2a and V2b INs. (A-D) Lateral views of 24 hpf *Tg(vsx1:GFP)* embryos. (A,B,K) The number of early-born V2a INs labeled with *vsx2* is unchanged in *lhx3+lhx4* MO-injected embryos. (C,D,K) The number of early-born V2b INs labeled with *tal1* is unchanged in *lhx3+lhx4* MO-injected embryos. (E-H) Lateral views of 2 dpf *Tg(vsx1:GFP)* embryos. (E,F) V2as labeled by GFP in 2 dpf *Tg(vsx2:EGFP)* embryos are reduced in *lhx3+lhx4* MO-injected embryos. (G,H) Single optical section; the number of V2bs co-labeled by *gata3* and GFP in *Tg(vsx1:GFP)* embryos is reduced in *lhx3+lhx4* MO-injected embryos. (I,J) Cross-section through mid-trunk of 2 dpf *Tg(vsx1:GFP)* embryos. The number of V2s and late p2 progenitors labeled by GFP is unaffected in *lhx3+lhx4* MO-injected embryos. Islet was included to exclude MNs that weakly express GFP (Reimer et al., 2013). (K) Quantification of early-born V2a and V2b INs (P>0.05; n=40 segments in ten embryos for each condition). (L) Quantification of V2a and V2b INs at 2 dpf (P_{V2a}=1×10^{-11}; P_{V2b}=2×10^{-5}; n=60 segments from ten embryos for each condition). (M) Quantification of V2 INs plus late p2 progenitors (P=0.14; n=10 alternating segments from ten embryos for each condition). In control embryos some weakly GFP$^+$ cells co-express Islet; these cells are MNs and were not included in p2 progenitor and V2 IN counts. Scale bars: 20 µm.

blocking MN characteristics within INs might be required under some circumstances. Whether or not transcription factors are deployed in VeLDs and KA′s to suppress MN characteristics remains unknown.

Strikingly, brachial MNs in *Lhx3 Lhx4* knockout mice convert to SAC MNs, the only class of spinal MN that normally lacks Lhx3 and Lhx4 expression (Sharma et al., 1998). SAC MNs are characterized by mediolateral soma positions and unusual lateral axon exit (Bravo-Ambrosio and Kaprielian, 2011). Our results in zebrafish show that, in the absence of Lhx3 and Lhx4, the few trunk motor axons that persist exit the spinal cord through the ventral root. These seemingly disparate results might be a consequence of the different axial levels analyzed. We restricted our analysis to spinal segments adjacent to somites 8-15. By comparison, Sharma et al. showed that Islet$^+$ MNs adjacent to cervical vertebrae 6-8 acquire features of SAC MNs, which are normally located adjacent to cervical vertebrae 1-5 (Sharma et al., 1998). DiI injection of dorsal axial muscles failed to label MNs at thoracic levels in double mutant mice, but the projections these presumptive MNs made was not described. We suspect that regional differences dictate the characteristics adopted by MNs in Lhx3- and Lhx4-deficient vertebrate embryos. MNs at cervical levels probably adopt an SAC MN fate, whereas those at more caudal levels probably acquire KA′ IN features. KA′s are best characterized in anamniotes (Bernhardt et al., 1992; Dale et al., 1987); however, similar cells were described in rats and primates (Stoeckel et al., 2003; Vigh et al., 2004). Definitive resolution of these differences will require further analysis of relationships among these neurons.

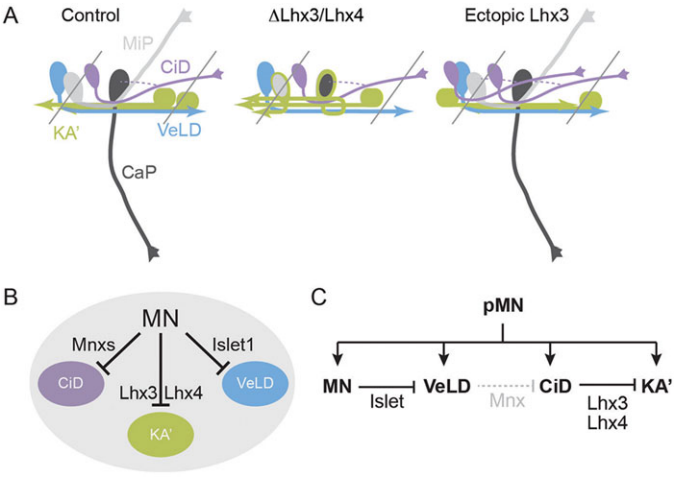

Fig. 8. Three transcription factor families prevent MNs from acquiring characteristics of specific pMN-derived INs. (A) In the absence of Lhx3 and Lhx4, MNs develop morphological and biochemical characteristics of KA′ INs. Forced expression of Lhx3 in pMN-derived neurons results in fewer KA′ INs, supernumerary CiDs and KA′ INs with descending axons. (B) Within MNs, Lhx3 and Lhx4 suppress acquisition of KA′ characteristics, Mnx family members suppress acquisition of CiD characteristics by MiP MNs and Islet1 suppresses acquisition of VeLD characteristics. (C) Among pMN domain neuronal derivatives, Lhx3 and Lhx4 segregate CiD from KA′ fates, and Islets segregate MN from VeLD fates. We hypothesize that Mnx contributes to segregation of VeLD from CiD fate, based on its role in blocking MiP from acquiring CiD characteristics.

Lhx3 segregates alternative fates of pMN-derived INs

Very little is known regarding fate segregation among pMN-derived INs. Our forced-expression experiments reveal that Lhx3 acts, at least in part, as a molecular switch to segregate CiD from KA′ fates. Our results and others (Appel et al., 1995; Batista et al., 2008) show that by 18 hpf Lhx3 is expressed in cells in addition to MNs in ventral neural tube; some of these cells are pMN-derived INs. This expression is maintained until at least 28 hpf. CiDs are derived from the pMN domain after 15 hpf, following PMN formation (Park et al., 2004). Together, these data indicate that Lhx3 is in the right place at the right time to promote CiD and inhibit KA′ fates. This idea is further corroborated by the differential ability of PMN

Development (2014) 141, 3900-3909 doi:10.1242/dev.105718

subtypes to acquire CiD features in the absence of Mnxs (Seredick et al., 2012) as a consequence of subtle but important differences in temporal expression of Islet transcription factors. CaPs express either Islet1 or Islet2a continuously. Thus, in the absence of Mnxs, they maintain expression of Islets and Lhxs and retain MN characteristics. By comparison, MiPs transiently downregulate Islet (Appel et al., 1995; Hutchinson et al., 2007; Hutchinson and Eisen, 2006). In the absence of Mnxs, MiPs temporarily express only Lhx during the Islet-negative period, the combinatorial code for CiDs, and can acquire a hybrid CiD phenotype.

We were surprised to find that Lhx3 and Lhx4 regulate expression of GABAergic properties in KA′s, although KA′s do not express Lhxs. This cell non-autonomous effect is not mediated via Notch signaling, the most obvious possibility (Shin et al., 2007). There are many other possible pathways, including electrical signaling through gap junctions. Most neurons within the developing zebrafish ventral spinal cord are electrically coupled through the first day of development (Saint-Amant and Drapeau, 2001; Wyart et al., 2009), and electrical activity has been shown to promote acquisition of transmitter phenotype (Spitzer, 2012). Lhx MO-injected embryos do not move properly at early developmental stages, perhaps as a result of disrupted activity of Lhx^+ MN and/or INs. It would be interesting to investigate this possibility in future experiments.

We show that all $Lhx3^+$ $Lhx4^+$ INs in the zebrafish spinal cord have descending axons, and that the intraspinal portion of the vast majority of MNs descend to the nearest adjacent ventral root. Even when forced expression of Lhx3 fails to drive CiD axon morphology in KA′s, it is often sufficient to redirect KA′ axons to extend into the caudal spinal cord. In mouse, forced expression of Lhx3 in $Mnx1^+$ MNs re-directs many axons into axial muscle at the expense of projections to normal targets in the limb, sympathetic ganglia and intercostal muscles (Sharma et al., 2000). One apparent target of Lhx3 overexpression is Fgfr1 (Shirasaki et al., 2006). Attraction to Fgf8 was proposed to set the axon trajectory of the $Lhx3^+$ medial motor column MNs that project to dermamyotome. Clearly, other signals contribute to medial motor column MN guidance at this choice point, as relatively few motor axons are misrouted in *Fgfr1* conditional mutants. It is intriguing to consider that an Fgf gradient established in the neural tube (Diez del Corral et al., 2003) might contribute to the descending pathways taken by these $Lhx3^+$ $Lhx4^+$ neurons.

Lhx3 and Lhx4 act together to specify late-developing V2 INs

Previous work in chick demonstrated sufficiency of Lhx3 in promoting expression of Vsx2, a V2a fate marker (Tanabe et al., 1998; Thaler et al., 2002). Our observations reveal that Lhx3 and Lhx4 are necessary for differentiation of both V2a and V2b INs, without affecting the number of immature V2 INs formed. Curiously, some V2a and V2b INs continue to be generated in Lhx3- and Lhx4-deficient embryos. In zebrafish, the first-born V2a and V2b pairs form independently of Lhx3 and Lhx4, as do a significant fraction of the V2a and V2b INs generated by 48 hpf. Although we cannot rule out that incomplete knockdown contributes to persistence of V2a and V2b INs at 48 hpf, there might be parallel or redundant mechanisms that cooperate with Lhx3 and Lhx4 to promote V2 IN specification. One attractive candidate is Bhlhe22 (previously Bhlhb5), an Olig-related transcription factor, the expression of which in V2 progenitors and V2a INs overlaps with Lhx3 (Skaggs et al., 2011). Reminiscent of our results after Lhx3 and Lhx4 knockdown, loss of Bhlhe22 function in chick reduced the number of V2a and V2b INs.

Interestingly, even after Lhx3 and Lhx4 knockdown, zebrafish embryos remain touch-responsive; however, they cannot sustain swimming through 4 dpf (data not shown). This is consistent with preservation of early-born V2a INs driving the highest-frequency movements during the initial phase of the escape response, and reduced numbers of later-born V2a INs driving lower-frequency movements during subsequent phases of the escape response (McLean and Fetcho, 2009). These observations suggest the exciting possibility that Lhx3 and Lhx4 coordinate development of subclasses of V2a INs underlying the circuitry responsible for setting locomotor speed, a question that remains to be addressed in future studies.

MATERIALS AND METHODS

Zebrafish lines

Wild-type, *Tg(nrp1a:GFP)*^{is12} (Sato-Maeda et al., 2008), *Tg(olig2:EGFP)*^{vu12} (Shin et al., 2003), *Tg(vsx1:GFP)*^{nns5} (Kimura et al., 2008), *Tg(vsx2:EGFP)*^{nns1} (Kimura et al., 2006) and *Et(-0.6hsp70l:GAL4VP16)*^{s1020t} (hereafter referred to as *s1020t*), *Tg(UAS-E1b:Kaede)*^{s1999t} (Wyart et al., 2009) zebrafish (*Danio rerio*) embryos were collected from natural crosses and staged by hours post fertilization at 28.5°C (hpf) and gross morphology (Kimmel et al., 1995). All experiments were carried out in accordance with animal welfare laws, guidelines and policies and were approved by the University of Oregon Institutional Animal Care and Use Committee.

Isolation of Lhx4

We isolated a full-length zebrafish *lhx4* transcript (1171 base pairs; 390 amino acids) from 24 hpf zebrafish cDNA using the following primers: forward 5′-CACACGGCGAAAGAACTCACG-3′; reverse 5′-TTTGCC-CACACCGAACACTG-3′. In phylogenetic analyses the protein encoded by this gene clusters with other Lhx4 proteins, not with Lhx3 proteins, indicating that it is an Lhx4 homolog (data not shown). Like other Lhx3 and Lhx4 proteins, zebrafish Lhx4 has two very highly conserved LIM domains as well as a highly conserved homeodomain.

Immunohistochemistry, RNA *in situ* hybridization and EdU labeling

Embryos were fixed and processed for *in situ* hybridization or antibody staining as previously described (Seredick et al., 2012). RNA probes include: *islet2a* and *lhx3* (Appel et al., 1995); *chat* (Tallafuss and Eisen, 2008); *tal1* and *gata3* (Batista et al., 2008); *vsx2* (Kimura et al., 2006); and *lhx4*. Primary antibodies include: mouse anti-Alcama (ZIRC, zn5; 1:4000); rabbit anti-GABA (Sigma, A2052; 1:1000); rabbit anti-Gad (Abcam, ab11070; 1:500); mouse anti-GFP (Clontech, 632381; 1:1000; or Life Technologies, A11120; 1:1000); rabbit anti-GFP (Life Technologies, A11122; 1:1000); mouse anti-phospho-Histone H3 (Abcam, ab14955; 1:1000); mouse anti-Islet (DSHB, 39.4D5; 1:1000); mouse anti-Syt2b (ZIRC, formerly znp1; 1:1000); mouse zn1 (ZIRC; 1:200).

To label proliferating cells, embryos were treated with 10 mM EdU solution (Click-iT EdU Alexa Fluor 555; Invitrogen, C10338) in embryo medium plus 15% DMSO for 20 min on ice. After rinsing into embryo medium, embryos recovered for 40 min and were fixed and processed by immunohistochemistry. Incorporated EdU was detected according to manufacturer's instructions.

Antibodies against Lhx3 and Lhx4 were generated by immunizing rabbits with truncated proteins corresponding to amino acids 237-397 of Lhx3 and 241-389 of Lhx4. We generated three antibodies: anti-Lhx3 antibody labels nuclei in ventral spinal cord and pituitary, the same cell population labeled by *lhx3* RNA probe. Anti-Lhx4 antibody labels fewer nuclei in ventral spinal cord than anti-Lhx3, as well as the pituitary and a dorsal IN population in the head, the same cell populations labeled by *lhx4* RNA probe. A third antibody labels as many nuclei in the ventral spinal cord as anti-Lhx3, as well as the pituitary and the dorsal INs in the head labeled by anti-Lhx4; we named this antibody anti-Lhx3/4.

Development (2014) 141, 3900-3909 doi:10.1242/dev.105718

Morpholino injections

One- to two-cell stage embryos were injected with 2.5 nl of translation-blocking MOs (GeneTools) targeting *lhx3* MO, 5′-GTTCTAAC-AACATTCTGGCGATAAA-3′ (125 µM), and/or *lhx4* MO, 5′-GCAG-CACAGCCGCACTTTGCATCAT-3′ (350 µM). *lhx3* and *lhx4* MO injection specifically eliminated expression of their respective proteins (supplementary material Fig. S2). MO specificity was confirmed using mis-match control MOs [*lhx3* MO 5-mis (5′-GTTGTAAGAACATT-GTGGCCATTAA-3′) and *lhx4* MO 5-mis (5′-GCACCACCCCGGA-CTTTCCATGAT-3′)] and rescue of the MN phenotype by mosaic overexpression of Lhx3. MO-injected embryos were morphologically normal and lacked elevated cell death assessed by Acridine Orange staining.

Mosaic labeling and Lhx3 overexpression within pMN-derived cells

To assess morphology of individual cells and determine proportions of pMN-derived neuronal classes, we injected *UAS:EGFPCAAX* or *UAS:EGFP-P2A-lhx3* DNA along with *Tol2 transposase* RNA into *s1020t* embryos. Synonymous substitutions in *lhx3* were introduced to prevent MO targeting of rescue RNA. Fluorescent embryos were selected and imaged live at 28-32 hpf. Alternatively, individual neurons in *lhx3* and *lhx4* MO-injected embryos were dye-labeled with 5% tetramethylrhodamine-dextran (D3308; Life Technologies) in 0.2 M KCl as previously described (Hale et al., 2011).

Microscopy

Images of embryos were captured on a Zeiss Axioplan using a digital camera, or a Zeiss Pascal confocal microscope. Adobe Photoshop was used to adjust image brightness and contrast.

Statistical analysis

Comparisons of means between groups were performed using two-sample unequal variance *t*-tests. An exact binomial test was used to assess changes in proportions of labeled MNs. Multiple comparisons were performed using a one-way ANOVA, followed by a post hoc Tukey–Kramer test. Analyses were performed using JMP 10 and Microsoft Excel. All data are reported as means±s.d.

Acknowledgements

We thank Chris Doe for comments on the manuscript. Joe Fetcho, Shin-Ichi Higashajima and Bruce Appel generously provided transgenic fish. The Islet monoclonal antibody developed by Thomas Jessell was obtained from the Developmental Studies Hybridoma Bank, developed under the auspices of the NICHD and maintained by The University of Iowa, Department of Biology, Iowa City, USA. We thank Ellie Melancon, Amanda Lewis, Jacob Lewis, Dayna Lamb and the University of Oregon Zebrafish Facility Staff for excellent fish husbandry and Ellie Melancon, Julia Ganz and Levi Simonson for help with some of the RNA *in situ* hybridization panels in Fig. 2.

Competing interests

The authors declare no competing financial interests.

Author contributions

S.S., S.A.H. and J.S.E. designed the study and wrote the draft manuscript, with contributions from L.V.R. and J.C.T. S.S., S.A.H., L.V.R., J.C.T. and J.S.E. all performed experiments for the study.

Funding

This work was supported by the National Institutes of Health (NIH) [NS23915 to J.S.E.; HD007348 to S.A.H. and L.V.R.]. Deposited in PMC for release after 12 months.

Supplementary material

Supplementary material available online at
http://dev.biologists.org/lookup/suppl/doi:10.1242/dev.105718/-/DC1

References

Appel, B. and Eisen, J. S. (1998). Regulation of neuronal specification in the zebrafish spinal cord by Delta function. *Development* **125**, 371-380.

Appel, B., Korzh, V., Glasgow, E., Thor, S., Edlund, T., Dawid, I. B. and Eisen, J. S. (1995). Motoneuron fate specification revealed by patterned LIM homeobox gene expression in embryonic zebrafish. *Development* **121**, 4117-4125.

Arber, S., Han, B., Mendelsohn, M., Smith, M., Jessell, T. M. and Sockanathan, S. (1999). Requirement for the homeobox gene Hb9 in the consolidation of motor neuron identity. *Neuron* **23**, 659-674.

Batista, M. F., Jacobstein, J. and Lewis, K. E. (2008). Zebrafish V2 cells develop into excitatory CiD and Notch signalling dependent inhibitory VeLD interneurons. *Dev. Biol.* **322**, 263-275.

Bernhardt, R. R., Chitnis, A. B., Lindamer, L. and Kuwada, J. Y. (1990). Identification of spinal neurons in the embryonic and larval zebrafish. *J. Comp. Neurol.* **302**, 603-616.

Bernhardt, R. R., Patel, C. K., Wilson, S. W. and Kuwada, J. Y. (1992). Axonal trajectories and distribution of GABAergic spinal neurons in wildtype and mutant zebrafish lacking floor plate cells. *J. Comp. Neurol.* **326**, 263-272.

Bravo-Ambrosio, A. and Kaprielian, Z. (2011). Crossing the border: molecular control of motor axon exit. *Int. J. Mol. Sci.* **12**, 8539-8561.

Dale, N., Roberts, A., Ottersen, O. P. and Storm-Mathisen, J. (1987). The morphology and distribution of 'Kolmer-Agduhr cells', a class of cerebrospinal-fluid-contacting neurons revealed in the frog embryo spinal cord by GABA immunocytochemistry. *Proc. R. Soc. Lond. B Biol. Sci.* **232**, 193-203.

Del Barrio, M. G., Taveira-Marques, R., Muroyama, Y., Yuk, D.-I., Li, S., Wines-Samuelson, M., Shen, J., Smith, H. K., Xiang, M., Rowitch, D. et al. (2007). A regulatory network involving Foxn4, Mash1 and delta-like 4/Notch1 generates V2a and V2b spinal interneurons from a common progenitor pool. *Development* **134**, 3427-3436.

Diez del Corral, R., Olivera-Martinez, I., Goriely, A., Gale, E., Maden, M. and Storey, K. (2003). Opposing FGF and retinoid pathways control ventral neural pattern, neuronal differentiation, and segmentation during body axis extension. *Neuron* **40**, 65-79.

Fashena, D. and Westerfield, M. (1999). Secondary motoneuron axons localize DM-GRASP on their fasciculated segments. *J. Comp. Neurol.* **406**, 415-424.

Gadd, M. S., Bhati, M., Jeffries, C. M., Langley, D. B., Trewhella, J., Guss, J. M. and Matthews, J. M. (2011). Structural basis for partial redundancy in a class of transcription factors, the LIM homeodomain proteins, in neural cell type specification. *J. Biol. Chem.* **286**, 42971-42980.

Haddon, C., Smithers, L., Schneider-Maunoury, S., Coche, T., Henrique, D. and Lewis, J. (1998). Multiple delta genes and lateral inhibition in zebrafish primary neurogenesis. *Development* **125**, 359-370.

Hale, L. A., Fowler, D. K. and Eisen, J. S. (2011). Netrin signaling breaks the equivalence between two identified zebrafish motoneurons revealing a new role of intermediate targets. *PLoS ONE* **6**, e25841.

Hutchinson, S. A. and Eisen, J. S. (2006). Islet1 and Islet2 have equivalent abilities to promote motoneuron formation and to specify motoneuron subtype identity. *Development* **133**, 2137-2147.

Hutchinson, S. A., Cheesman, S. E., Hale, L. A., Boone, J. Q. and Eisen, J. S. (2007). Nkx6 proteins specify one zebrafish primary motoneuron subtype by regulating late islet1 expression. *Development* **134**, 1671-1677.

Joshi, K., Lee, S., Lee, B., Lee, J. W. and Lee, S.-K. (2009). LMO4 controls the balance between excitatory and inhibitory spinal V2 interneurons. *Neuron* **61**, 839-851.

Kimmel, C. B., Ballard, W. W., Kimmel, S. R., Ullmann, B. and Schilling, T. F. (1995). Stages of embryonic development of the zebrafish. *Dev. Dyn.* **203**, 253-310.

Kimura, Y., Okamura, Y. and Higashijima, S.-i. (2006). alx, a zebrafish homolog of Chx10, marks ipsilateral descending excitatory interneurons that participate in the regulation of spinal locomotor circuits. *J. Neurosci.* **26**, 5684-5697.

Kimura, Y., Satou, C. and Higashijima, S.-i. (2008). V2a and V2b neurons are generated by the final divisions of pair-producing progenitors in the zebrafish spinal cord. *Development* **135**, 3001-3005.

Korzh, V., Edlund, T. and Thor, S. (1993). Zebrafish primary neurons initiate expression of the LIM homeodomain protein Isl-1 at the end of gastrulation. *Development* **118**, 417-425.

Kuwada, J. Y., Bernhardt, R. R. and Chitnis, A. B. (1990). Pathfinding by identified growth cones in the spinal cord of zebrafish embryos. *J. Neurosci.* **10**, 1299-1308.

Lee, S.-K. and Pfaff, S. L. (2003). Synchronization of neurogenesis and motor neuron specification by direct coupling of bHLH and homeodomain transcription factors. *Neuron* **38**, 731-745.

Lee, S., Lee, B., Joshi, K., Pfaff, S. L., Lee, J. W. and Lee, S.-K. (2008). A regulatory network to segregate the identity of neuronal subtypes. *Dev. Cell* **14**, 877-889.

Lee, S., Lee, B., Lee, J. W. and Lee, S.-K. (2009). Retinoid signaling and neurogenin2 function are coupled for the specification of spinal motor neurons through a chromatin modifier CBP. *Neuron* **62**, 641-654.

Lee, S., Cuvillier, J. M., Lee, B., Shen, R., Lee, J. W. and Lee, S.-K. (2012). Fusion protein Isl1-Lhx3 specifies motor neuron fate by inducing motor neuron genes and concomitantly suppressing the interneuron programs. *Proc. Natl. Acad. Sci. USA* **109**, 3383-3388.

Lewis, K. E. (2006). How do genes regulate simple behaviours? Understanding how different neurons in the vertebrate spinal cord are genetically specified. *Philos. Trans. R. Soc. Lond. B Biol. Sci.* **361**, 45-66.

Lewis, K. E. and Eisen, J. S. (2003). From cells to circuits: development of the zebrafish spinal cord. *Prog. Neurobiol.* **69**, 419-449.

Li, H., Witte, D. P., Branford, W. W., Aronow, B. J., Weinstein, M., Kaur, S., Wert, S., Singh, G., Schreiner, C. M., Whitsett, J. A. et al. (1994). Gsh-4 encodes a LIM-type homeodomain, is expressed in the developing central nervous system and is required for early postnatal survival. *EMBO J.* **13**, 2876-2885.

Lundfald, L., Restrepo, C. E., Butt, S. J. B., Peng, C.-Y., Droho, S., Endo, T., Zeilhofer, H. U., Sharma, K. and Kiehn, O. (2007). Phenotype of V2-derived interneurons and their relationship to the axon guidance molecule EphA4 in the developing mouse spinal cord. *Eur. J. Neurosci.* **26**, 2989-3002.

McLean, D. L. and Fetcho, J. R. (2008). Using imaging and genetics in zebrafish to study developing spinal circuits in vivo. *Dev. Neurobiol.* **68**, 817-834.

McLean, D. L. and Fetcho, J. R. (2009). Spinal interneurons differentiate sequentially from those driving the fastest swimming movements in larval zebrafish to those driving the slowest ones. *J. Neurosci.* **29**, 13566-13577.

Melancon, E., Liu, D. W., Westerfield, M. and Eisen, J. S. (1997). Pathfinding by identified zebrafish motoneurons in the absence of muscle pioneers. *J. Neurosci.* **17**, 7796-7804.

Myers, P. Z., Eisen, J. S. and Westerfield, M. (1986). Development and axonal outgrowth of identified motoneurons in the zebrafish. *J. Neurosci.* **6**, 2278-2289.

Park, H.-C., Shin, J. and Appel, B. (2004). Spatial and temporal regulation of ventral spinal cord precursor specification by Hedgehog signaling. *Development* **131**, 5959-5969.

Peng, C.-Y., Yajima, H., Burns, C. E., Zon, L. I., Sisodia, S. S., Pfaff, S. L. and Sharma, K. (2007). Notch and MAML signaling drives Scl-dependent interneuron diversity in the spinal cord. *Neuron* **53**, 813-827.

Pfaff, S. L., Mendelsohn, M., Stewart, C. L., Edlund, T. and Jessell, T. M. (1996). Requirement for LIM homeobox gene Isl1 in motor neuron generation reveals a motor neuron-dependent step in interneuron differentiation. *Cell* **84**, 309-320.

Reimer, M. M., Norris, A., Ohnmacht, J., Patani, R., Zhong, Z., Dias, T. B., Kuscha, V., Scott, A. L., Chen, Y.-C., Rozov, S. et al. (2013). Dopamine from the brain promotes spinal motor neuron generation during development and adult regeneration. *Dev. Cell* **25**, 478-491.

Saint-Amant, L. and Drapeau, P. (2001). Synchronization of an embryonic network of identified spinal interneurons solely by electrical coupling. *Neuron* **31**, 1035-1046.

Sato-Maeda, M., Obinata, M. and Shoji, W. (2008). Position fine-tuning of caudal primary motoneurons in the zebrafish spinal cord. *Development* **135**, 323-332.

Seredick, S. D., Van Ryswyk, L., Hutchinson, S. A. and Eisen, J. S. (2012). Zebrafish Mnx proteins specify one motoneuron subtype and suppress acquisition of interneuron characteristics. *Neural Dev.* **7**, 35.

Sharma, K., Sheng, H. Z., Lettieri, K., Li, H., Karavanov, A., Potter, S., Westphal, H. and Pfaff, S. L. (1998). LIM homeodomain factors Lhx3 and Lhx4 assign subtype identities for motor neurons. *Cell* **95**, 817-828.

Sharma, K., Leonard, A. E., Lettieri, K. and Pfaff, S. L. (2000). Genetic and epigenetic mechanisms contribute to motor neuron pathfinding. *Nature* **406**, 515-519.

Sheng, H. Z., Zhadanov, A. B., Mosinger, B.Jr, Fujii, T., Bertuzzi, S., Grinberg, A., Lee, E. J., Huang, S.-P., Mahon, K. A. and Westphal, H. (1996). Specification of pituitary cell lineages by the LIM homeobox gene Lhx3. *Science* **272**, 1004-1007.

Shin, J., Park, H.-C., Topczewska, J. M., Mawdsley, D. J. and Appel, B. (2003). Neural cell fate analysis in zebrafish using olig2 BAC transgenics. *Methods Cell Sci.* **25**, 7-14.

Shin, J., Poling, J., Park, H.-C. and Appel, B. (2007). Notch signaling regulates neural precursor allocation and binary neuronal fate decisions in zebrafish. *Development* **134**, 1911-1920.

Shirasaki, R., Lewcock, J. W., Lettieri, K. and Pfaff, S. L. (2006). FGF as a target-derived chemoattractant for developing motor axons genetically programmed by the LIM code. *Neuron* **50**, 841-853.

Skaggs, K., Martin, D. M. and Novitch, B. G. (2011). Regulation of spinal interneuron development by the Olig-related protein Bhlhb5 and Notch signaling. *Development* **138**, 3199-3211.

Spitzer, N. C. (2012). Activity-dependent neurotransmitter respecification. *Nat. Rev. Neurosci.* **13**, 94-106.

Stifani, N., Freitas, A. R. O., Liakhovitskaia, A., Medvinsky, A., Kania, A. and Stifani, S. (2008). Suppression of interneuron programs and maintenance of selected spinal motor neuron fates by the transcription factor AML1/Runx1. *Proc. Natl. Acad. Sci. USA* **105**, 6451-6456.

Stoeckel, M.-E., Uhl-Bronner, S., Hugel, S., Veinante, P., Klein, M.-J., Mutterer, J., Freund-Mercier, M.-J. and Schlichter, R. (2003). Cerebrospinal fluid-contacting neurons in the rat spinal cord, a gamma-aminobutyric acidergic system expressing the P2X2 subunit of purinergic receptors, PSA-NCAM, and GAP-43 immunoreactivities: light and electron microscopic study. *J. Comp. Neurol.* **457**, 159-174.

Tallafuss, A. and Eisen, J. S. (2008). The Met receptor tyrosine kinase prevents zebrafish primary motoneurons from expressing an incorrect neurotransmitter. *Neural Dev.* **3**, 18.

Tanabe, Y., William, C. and Jessell, T. M. (1998). Specification of motor neuron identity by the MNR2 homeodomain protein. *Cell* **95**, 67-80.

Thaler, J., Harrison, K., Sharma, K., Lettieri, K., Kehrl, J. and Pfaff, S. L. (1999). Active suppression of interneuron programs within developing motor neurons revealed by analysis of homeodomain factor HB9. *Neuron* **23**, 675-687.

Thaler, J. P., Lee, S.-K., Jurata, L. W., Gill, G. N. and Pfaff, S. L. (2002). LIM factor Lhx3 contributes to the specification of motor neuron and interneuron identity through cell-type-specific protein-protein interactions. *Cell* **110**, 237-249.

Thor, S., Andersson, S. G. E., Tomlinson, A. and Thomas, J. B. (1999). A LIM-homeodomain combinatorial code for motor-neuron pathway selection. *Nature* **397**, 76-80.

Trevarrow, B., Marks, D. L. and Kimmel, C. B. (1990). Organization of hindbrain segments in the zebrafish embryo. *Neuron* **4**, 669-679.

Tsuchida, T., Ensini, M., Morton, S. B., Baldassare, M., Edlund, T., Jessell, T. M. and Pfaff, S. L. (1994). Topographic organization of embryonic motor neurons defined by expression of LIM homeobox genes. *Cell* **79**, 957-970.

Vallstedt, A., Muhr, J., Pattyn, A., Pierani, A., Mendelsohn, M., Sander, M., Jessell, T. M. and Ericson, J. (2001). Different levels of repressor activity assign redundant and specific roles to Nkx6 genes in motor neuron and interneuron specification. *Neuron* **31**, 743-755.

Vigh, B., Manzano e Silva, M. J., Frank, C. L., Vincze, C., Czirok, S. J., Szabo, A., Lukats, A. and Szel, A. (2004). The system of cerebrospinal fluid-contacting neurons. Its supposed role in the nonsynaptic signal transmission of the brain. *Histol. Histopathol.* **19**, 607-628.

Wyart, C., Del Bene, F., Warp, E., Scott, E. K., Trauner, D., Baier, H. and Isacoff, E. Y. (2009). Optogenetic dissection of a behavioural module in the vertebrate spinal cord. *Nature* **461**, 407-410.

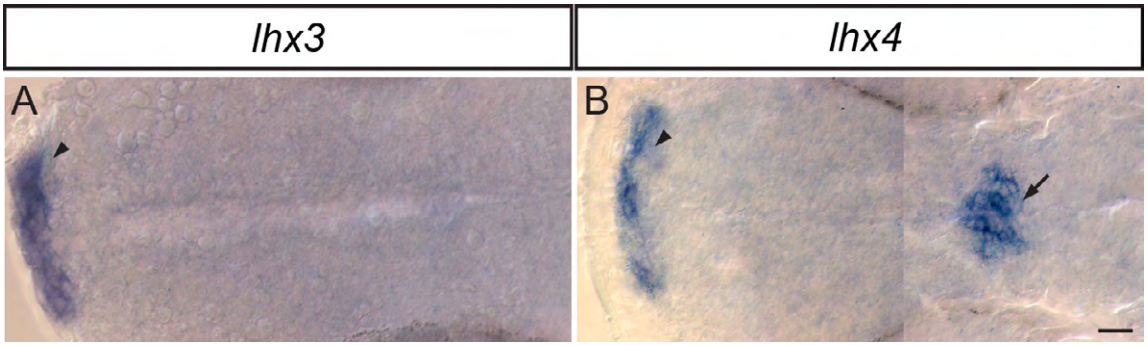

Supplemental Figure S1. Lhx3 and Lhx4 are expressed in the anterior central nervous system
(A,B) Dorsal views of 24 hpf embryos labeled for *lhx3* (A) and *lhx4* (B). *lhx3* and *lhx4* both label the pituitary (arrowhead), while *lhx4* additionally labels a dorsal population of INs between the eyes (arrow).

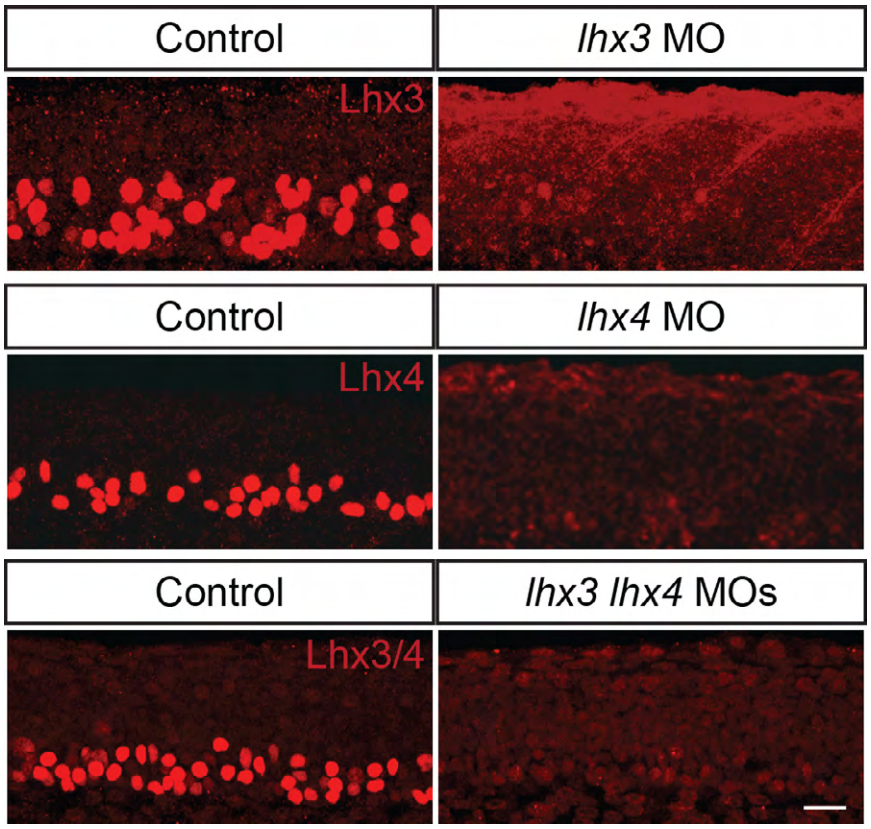

Supplemental Figure S2. Morpholinos targeting *lhx3* and *lhx4* block translation
Lateral views of 24 hpf embryos. (A,B) Embryos injected with *lhx3* MO lack Lhx3 protein. (C,D) Embryos injected with *lhx4* MO lack Lhx4 protein. (E,F) Embryos injected with *lhx3* plus *lhx4* MOs lack both Lhx3 and Lhx4 protein. Scale bar: 20 μm.

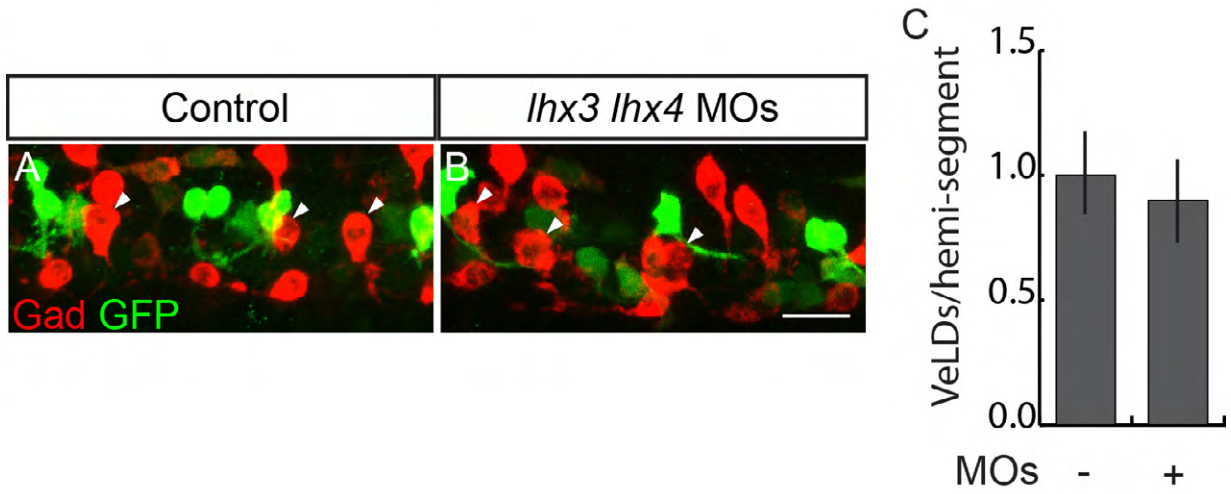

Supplemental Figure S3. Lhx3 and Lhx4 do not regulate VeLD IN specification
(A,B) Lateral views of 20 hpf *Tg(vsx1:GFP)* embryos co-labeled for GFP and Gad. VeLDs (arrowheads) persist in embryos injected with *lhx3* plus *lhx4* MOs. (C) Quantification of VeLDs (n = 50 segments in 10 embryos per condition). Scale bar: 20 μm.

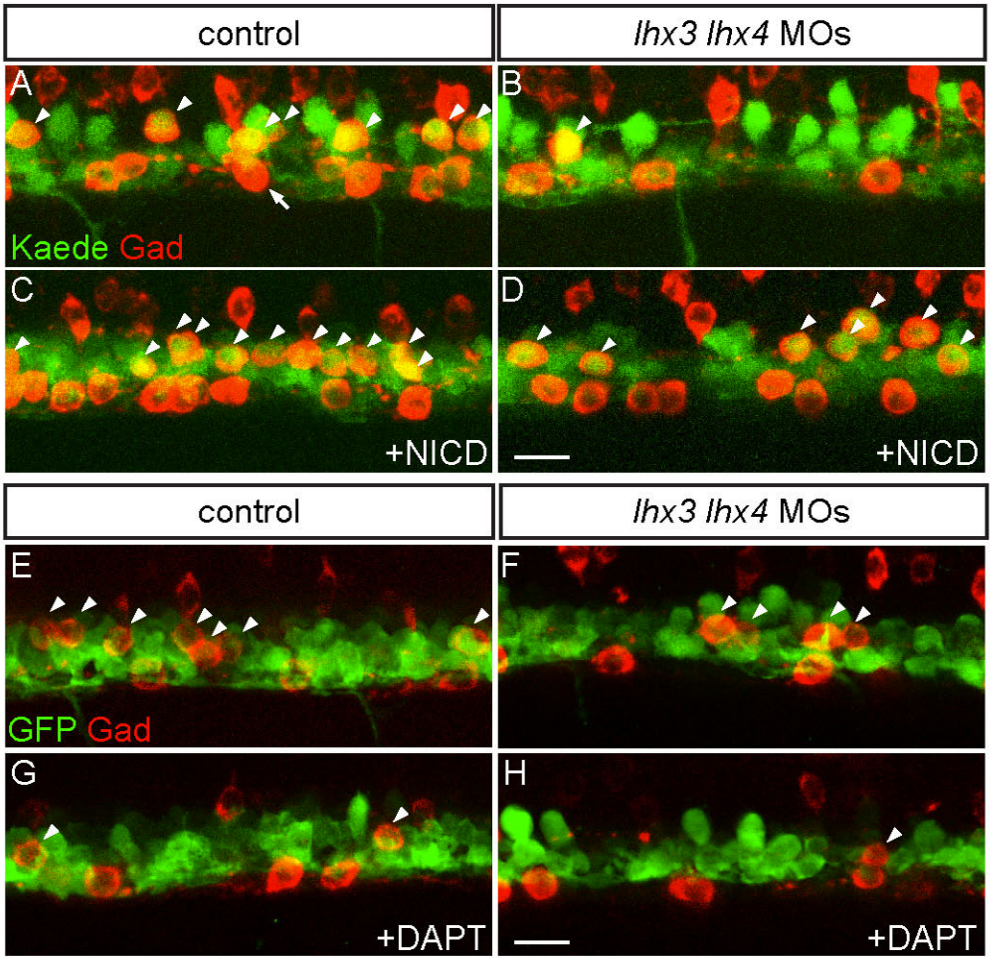

I

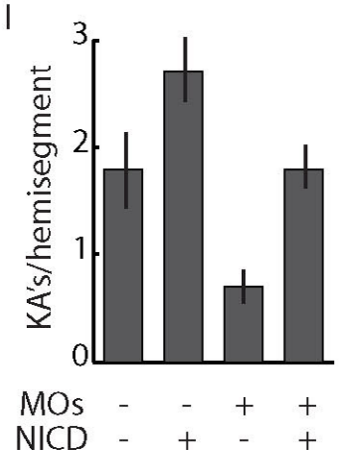

	UIC	UIC, NICD	MO	MO, NICD
UIC		$5x10^{-3}$	$<1x10^{-4}$	0.98
UIC, NICD			$<1x10^{-4}$	$2x10^{-3}$
MO				$3x10^{-4}$
MO, NICD				

J

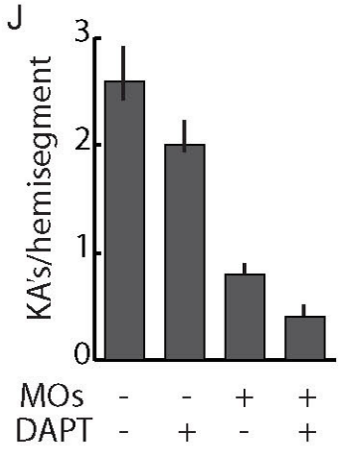

	UIC	UIC, DAPT	MO	MO, DAPT
UIC		$1x10^{-3}$	$<1x10^{-4}$	$<1x10^{-4}$
UIC, DAPT			$<1x10^{-4}$	$<1x10^{-4}$
MO				0.019
MO, DAPT				

Supplemental Figure S4. Lhx3 and Lhx4 cell non-autonomously promote KA'differentiation independently of Notch signaling

(A-D) Lateral views of 24 hpf *s1020t;Tg(UAS-E1b:Kaede)* embryos labeled for Gad. (A) KA's form a row of Gad^+ $Kaede^+$ cells in the most dorsal portion of the Kaede expression domain (arrowheads); the more ventral row of Gad^+ $Kaede^-$ cells in each panel are p3-derived KA" INs (arrow). (B) Very few KA's express Gad in *lhx3* plus *lhx4* MO-injected embryos. (C) Expression of NICD significantly increased the number of KA's. (D) Expression of NICD in *lhx3* plus *lhx4* MO-injected embryos increased the number of KA's expressing Gad to control levels. (E-H) Lateral views of 28 hpf *Tg(olig2:GFP)* embryos labeled for Gad and GFP. (E) KA's (arrowheads) are visible as a row of Gad^+ cells at the dorsalmost region labeled by GFP. GFP is rapidly extinguished from post-mitotic KA's. (F) Very few KA's express Gad (arrowheads) in *lhx3* plus *lhx4* MO-injected embryos. (G) Application of 50 μM DAPT at 6 hpf reduced the number of KA's relative to control embryos. (H) Application of 50 μM DAPT at 6 hpf to *lhx3* plus *lhx4* MO-injected embryos further reduced the number of KA's. (I) Quantification of KA' numbers after Notch activation. (J) Quantification of KA' numbers after Notch inhibition. (I,J) One-way ANOVA, $p<1x10^{-4}$; *post hoc* comparisons using Tukey-Kramer HSD for all pairwise combinations are presented as p-values in the adjoining table. Scale bar: 20 μm.